Green Chemistry

PAPER

Check for updates

Synergistic co-upcycling of polycarbonate and organophosphate ester wastes *via* chemically complementary reactivity

Yunkai Yu,†[a,b] Zexiang Wu,†[a,b] Minghao Zhang,†[a,b] Siyu Zhang,[a,b] Yanwen Wang,[a,b] Jing Li,[c,d] Weixiang Wu[a,b] and Qingqing Mei ⭐[a,b]

The concurrent accumulation of polycarbonate (PC) plastic and organophosphate ester (OPE) wastes poses a persistent environmental challenge as these chemically distinct hazardous streams are conventionally managed through separate, energy-intensive treatment pathways that result in resource loss and secondary pollution. Herein, we report a synergistic co-upcycling strategy that chemically couples these two waste streams within a single catalytic process, transforming them into value-added chemicals with reduced environmental and health risks. Using mild carbonate catalysts, the complete depolymerization of PC is achieved concurrently with selective alkylation of the released bisphenol A (BPA), with OPEs serving as *in situ* alkylating agents. This one-pot process exhibits broad substrate generality across diverse commercial PC wastes and OPEs, affording bisphenol A alkyl ethers in high yields (92%–99%). The approach also remains effective in chemically complex matrices representative of industrial waste streams, including trioctyl phosphate solvent waste from anthraquinone-based hydrogen peroxide production and tributyl phosphate extraction waste from metallurgical solvent-extraction operations. A distinguishing feature is the controlled mono-dealkylation of OPEs, exemplified by the quantitative conversion of trimethyl phosphate into dimethyl phosphate, a valuable industrial intermediate, without over-dealkylation. This work demonstrates a waste-to-waste co-upcycling approach that leverages chemical complementarity between two hazardous waste streams to reduce environmental burdens while recovering chemical value.

Green foundation

1. This work advances green chemistry by establishing a waste-to-waste co-upcycling paradigm that chemically couples two hazardous waste streams, polycarbonate (PC) plastics and organophosphate esters (OPEs), within a single integrated process. By exploiting their intrinsic chemical complementarity, this strategy transforms conventionally incompatible solid and liquid wastes into mutually enabling resources, demonstrating a systems-level approach to hazardous waste valorization beyond single-stream recycling.

2. This work demonstrates a synergistic co-upcycling process that simultaneously converts PC and OPE wastes into value-added chemicals with high efficiency and intrinsic selectivity. The system affords bisphenol A alkyl ethers in consistently high yields (92%–99%) while achieving 100% selective mono-dealkylation of phosphate esters without over-dealkylation. This inherent reaction control suppresses secondary byproducts, simplifies separation, and enables concurrent recovery of two industrially relevant products from hazardous waste streams. The approach maximizes resource efficiency while minimizing secondary pollution.

3. Future research studies could further enhance the sustainability of this system by replacing polar aprotic solvents with greener alternatives, reducing reaction temperature through catalyst optimization, and integrating continuous-flow processing for improved energy efficiency.

[a]State Key Laboratory of Soil Pollution Control and Safety, Zhejiang University, Hangzhou, 310058 Zhejiang, China. E-mail: meiqq@zju.edu.cn
[b]Institute of Environment Science and Technology, College of Environmental and Resource Sciences, Zhejiang University, Hangzhou, 310058 Zhejiang, China
[c]Key Laboratory of Biomass Chemical Engineering of Ministry of Education, College of Chemical and Biological Engineering, Zhejiang University, Hangzhou, 310058 Zhejiang, China
[d]Institute of Zhejiang University-Quzhou, 99 Zheda Road, Quzhou, 324000 Zhejiang, China
† These authors contributed equally.

1. Introduction

The global accumulation of plastic waste presents a persistent environmental challenge, driven by increasing production, limited recycling capacity, and the long environmental lifetimes of synthetic polymers.[1–4] Among engineering plastics, polycarbonate (PC) is of particular concern due to its widespread use in electronics, construction, and optical materials, as well as its reliance on bisphenol A (BPA) as a structural

monomer.[5,6] Most post-consumer PC is currently landfilled or incinerated,[7,8] which not only wastes its material value but also risks releasing BPA, a well-established endocrine-disrupting compound with documented ecological and human health impacts.

Chemical recycling strategies, including hydrolysis[9,10] and alcoholysis[11,12] (Tables S1 and S2), have been developed to depolymerize PC and recover BPA. However, these approaches share a fundamental limitation: the primary product, BPA, retains its intrinsic toxicity and faces increasingly stringent regulatory restrictions,[13] substantially constraining its reuse and market value. As a result, conventional PC recycling often amounts to molecular-level recovery without meaningful risk mitigation. Transforming BPA into safer, higher-value derivatives has therefore emerged as a critical objective for sustainable PC waste management,[14–17] yet existing methods typically depend on externally supplied alkylating reagents (*e.g.*, alkyl carbonate,[18] iodomethane,[19] and dimethyl sulfate[20]), introducing additional economic and environmental burdens.

In parallel, organophosphate esters (OPEs) have emerged as a pervasive class of environmental contaminants.[21–23] Widely employed as functional solvents, flame retardants, plasticizers, and hydraulic fluids, OPEs are produced at large scales and are characterized by environmental persistence and potential toxicity.[24–26] Current remediation strategies, including advanced oxidation, adsorption, membrane separation, and biodegradation, are primarily designed for dilute aqueous systems and are poorly suited for treating high-concentration OPE waste streams generated in industrial settings.[27–29] Moreover, such methods often involve high operational costs and may generate secondary pollution. Importantly, these strategies emphasize pollutant removal rather than resource recovery, resulting in a significant loss of potentially valuable chemical resources. Consequently, significant volumes of concentrated OPE wastes accumulate in industrial settings, representing both an environmental liability and a lost chemical resource.

Despite their co-occurrence in industrial and consumer product life cycles, PC plastics and OPEs are conventionally treated as fundamentally incompatible waste streams, solid polymer waste *versus* liquid hazardous organics, which requires separate treatment infrastructures and regulatory pathways. This compartmentalized approach leads to duplicated energy input, inefficient resource utilization, and persistent secondary pollution. This separation reflects a conceptual and regulatory convention rather than a chemical necessity. Upon depolymerization, PC constitutes a reservoir of nucleophilic phenolate species, while OPEs possess electrophilic alkyl groups capable of substitution reactions. Strategically coupling these complementary functionalities offers an opportunity to transform two problematic wastes into mutually enabling resources.

In this study, we report a one-pot catalytic strategy for the synergistic co-upcycling of PC plastics and OPE wastes into value-added bisphenol A alkyl ethers and partially dealkylated phosphates (Fig. 1). Using mild carbonate catalysts, PC depoly-

merization and BPA alkylation are integrated into a single process, with OPEs serving as *in situ* alkylating agents. The strategy demonstrates broad applicability across diverse commercial PC wastes and OPE substrates and is further validated using chemically complex industrial waste streams, including the trioctyl phosphate (TOP)-based solvent waste from the anthraquinone-based hydrogen peroxide (H_2O_2) production process and tributyl phosphate (TBP)-based extraction waste from metallurgical solvent-extraction operations. This synergistic strategy eliminates the need for external alkylating reagents, enhances resource utilization by simultaneously converting two waste streams and upgrades BPA into higher-value alkyl ether derivatives. By demonstrating that chemically complementary hazardous wastes can be co-converted rather than treated in isolation, this work establishes a practical example for exploiting chemical compatibility between waste streams toward more efficient and sustainable recycling.

2. Materials and methods

### 2.1 General procedure for PC-OPE co-upcycling

In a typical reaction, PC pellets (1 mmol monomer unit), cesium carbonate (Cs_2CO_3, 3 mmol), trimethyl phosphate (3 mmol), and *N,N*-dimethylformamide (DMF, 2 mL) were added to a 15 mL thick-walled pressure-resistant vial equipped with a magnetic stirrer. The sealed vial was immersed in an oil bath preheated to 100 °C and stirred at 600 rpm for 30 min. Upon completion, the reaction vial was immediately transferred to an ice-water bath and cooled to room temperature. Mesitylene (1 mmol, 120 mg) was added as an internal standard, followed by 10 mL ethyl acetate and 6 mL HCl (1 mol L^{-1}) for acidification and extraction. The organic phase was analyzed by gas chromatography (GC) to determine the product yields.

The co-upcycling methodology was successfully applied to various phosphate ester substrates, including triethyl phosphate, tripropyl phosphate, tributyl phosphate, triallyl phosphate, tris(2-butoxyethyl) phosphate, and tris(2-ethylhexyl) phosphate, following the general procedure, with the specific temperature adjustments provided in the caption of Fig. 2. Product yields for different bisphenol A alkyl ethers were quantified by ^{1}H NMR spectroscopy using mesitylene (1 mmol) as an internal standard.

2.2 Preparation of simulated industrial OPE waste liquids

Simulated OPE waste liquids were prepared to represent realistic compositions of industrial solvent residues while ensuring compositional reproducibility. These formulations were designed to capture the chemical complexity of representative industrial waste streams without relying on site-specific samples, thereby enabling controlled and systematic evaluation. The simulated TOP-based waste liquid, representative of solvent residues generated during the anthraquinone-based H_2O_2 production process, was prepared as a homogeneous mixture containing TOP (59.2 mmol), 2-ethylanthraquinone
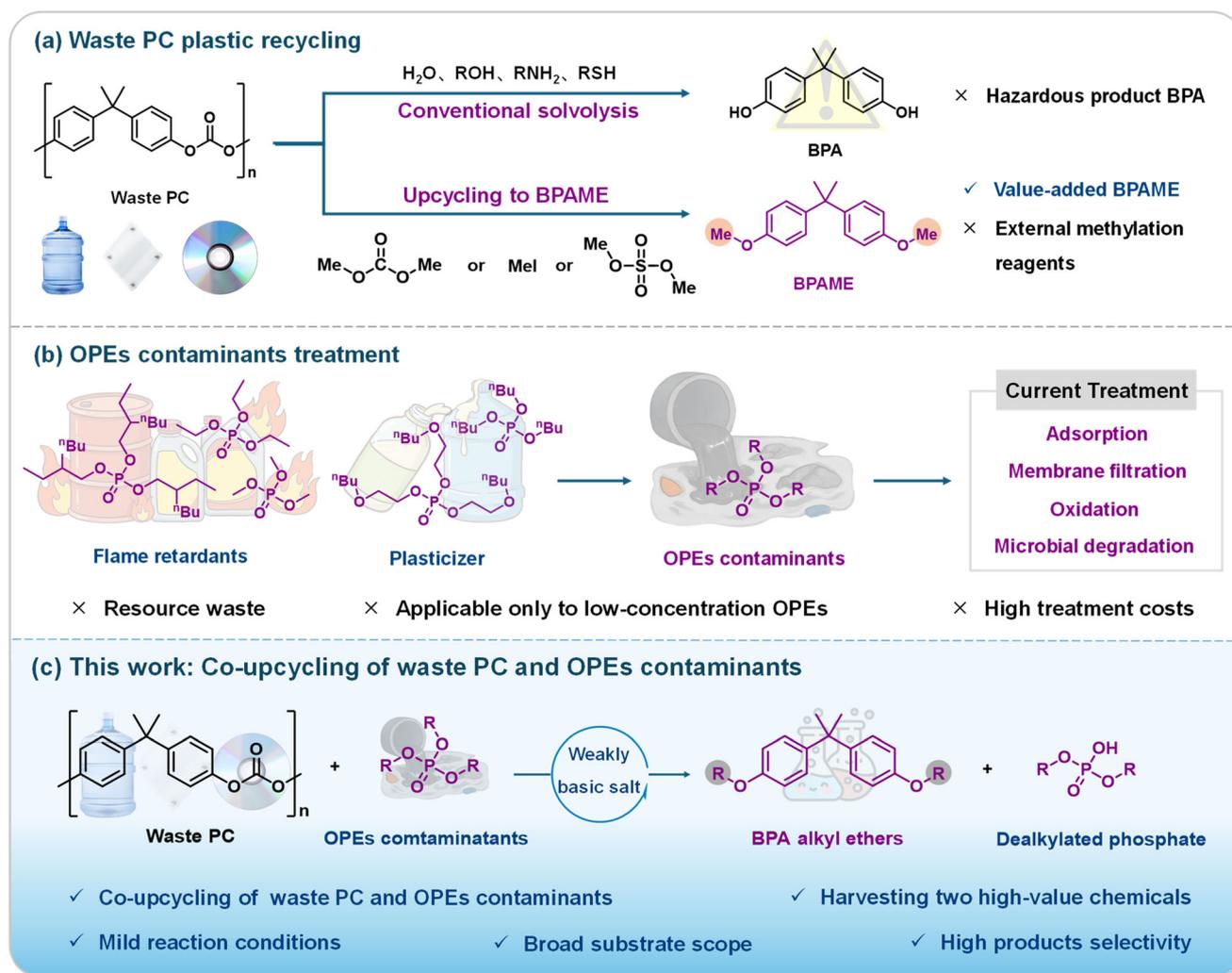
Fig. 1 Treatment of waste PC and OPE contaminants. (a) Conventional PC plastic waste recycling routes. (b) Existing treatment strategies for OPE contaminants. (c) This work: synergistic co-upcycling of waste PC and OPE contaminants into high-value tailored bisphenol A alkyl ethers and partially dealkylated phosphates.

(5.92 mmol), *p*-xylene (3.7 mmol), cumene (3.7 mmol), and tetrabutylurea (1.48 mmol), with a total mass of 28.44 g. The simulated TBP-containing extraction waste liquid, representative of solvent-extraction residues from metallurgical processing, was prepared as a homogeneous mixture containing TBP (905 mmol), *n*-dodecane (225 mmol), dibutyl phosphate (78.7 mmol), monobutyl phosphate (22.5 mmol), and zirconium *n*-propanolate (11.2 mmol), with a total mass of 286.5 g.

2.3 Characterization

The product yield was analyzed by gas chromatography (GC, Agilent 8860, with Agilent J & W HP-5 polysiloxane gas chromatography column) and gas chromatography-mass spectrometry (GC-MS, Agilent 7890A/5975C GC/MSD, with Agilent J&W HP-5 Polysiloxane GC Column). Nuclear magnetic resonance (NMR) spectra were recorded at room temperature using a Bruker Avance-600 instrument (^{1}H NMR at 600 MHz, ^{13}C NMR at 151 MHz and ^{31}P NMR at 243 MHz).

Density functional theory (DFT) calculations were performed using the Gaussian 16 software.[30] Geometry optimizations were carried out at the B3LYP/6-311+G** level[31–34] with the SMD solvation model.[35,36] All optimized structures were verified by frequency calculations, and only one imaginary frequency was found in the transition states, while the other structures had no imaginary frequency. Besides, the thermal correction to Gibbs free energy was obtained after frequency calculations. Intrinsic Reaction Coordinate (IRC)[37] was utilized to confirm the reaction pathway.

3. Results and discussion

3.1 Co-upcycling of PC with diverse OPEs

We initially established the reaction conditions using PC and trimethyl phosphate (TMP) as a model system (sections S3 and S4 in SI). Systematic screening of bases revealed Cs_2CO_3 as the

most effective catalyst. Under optimized conditions (DMF, 100 °C, 30 min), complete depolymerization of PC was achieved, affording bisphenol A dimethyl ether (BPAME) in 99% yield. Parametric studies confirmed that solvent polarity, temperature, and reaction time play key roles in facilitating PC depolymerization and subsequent alkylation.

Evaluation of substrate scope revealed broad compatibility with structurally diverse OPEs (Fig. 2). Methyl phosphate esters generally afforded BPAME in yields exceeding 81% under standard conditions. Trimethyl phosphite (P(OMe)$_3$) initially exhibited lower reactivity, consistent with the absence of a P=O bond and the resulting reduced O–Me polarity;[38] however, increasing the temperature to 140 °C improved the yield to 93%. Higher alkyl phosphate esters, including ethyl, propyl, and butyl phosphates (3b–3d), required elevated temperatures but were efficiently converted to the corresponding

bisphenol A alkyl ethers. This flexibility is important for practical deployment, as it allows the process to be tailored to specific, variable waste compositions encountered in industrial applications, moving beyond idealized model systems.

The co-upcycling strategy is directly applicable to PC materials containing authentic, commercially used phosphorus-based additives (Fig. 2b). Triallyl phosphate (TAP, 3e) was selectively transformed to bisphenol A diallyl ether in 99% yield, a compound of direct industrial relevance as a precursor for epoxy resins used in coatings and composite materials.[39,40] When a PC incorporating tris(2-butoxyethyl) phosphate plasticizer (3f)[41] or tris(2-ethylhexyl) phosphate flame retardant (3g)[42] was directly processed, the corresponding bisphenol A alkyl ethers were obtained in 93% and 95% yields, respectively. These results demonstrate that phosphate-based additives, which are conventionally viewed as contaminants that compli-
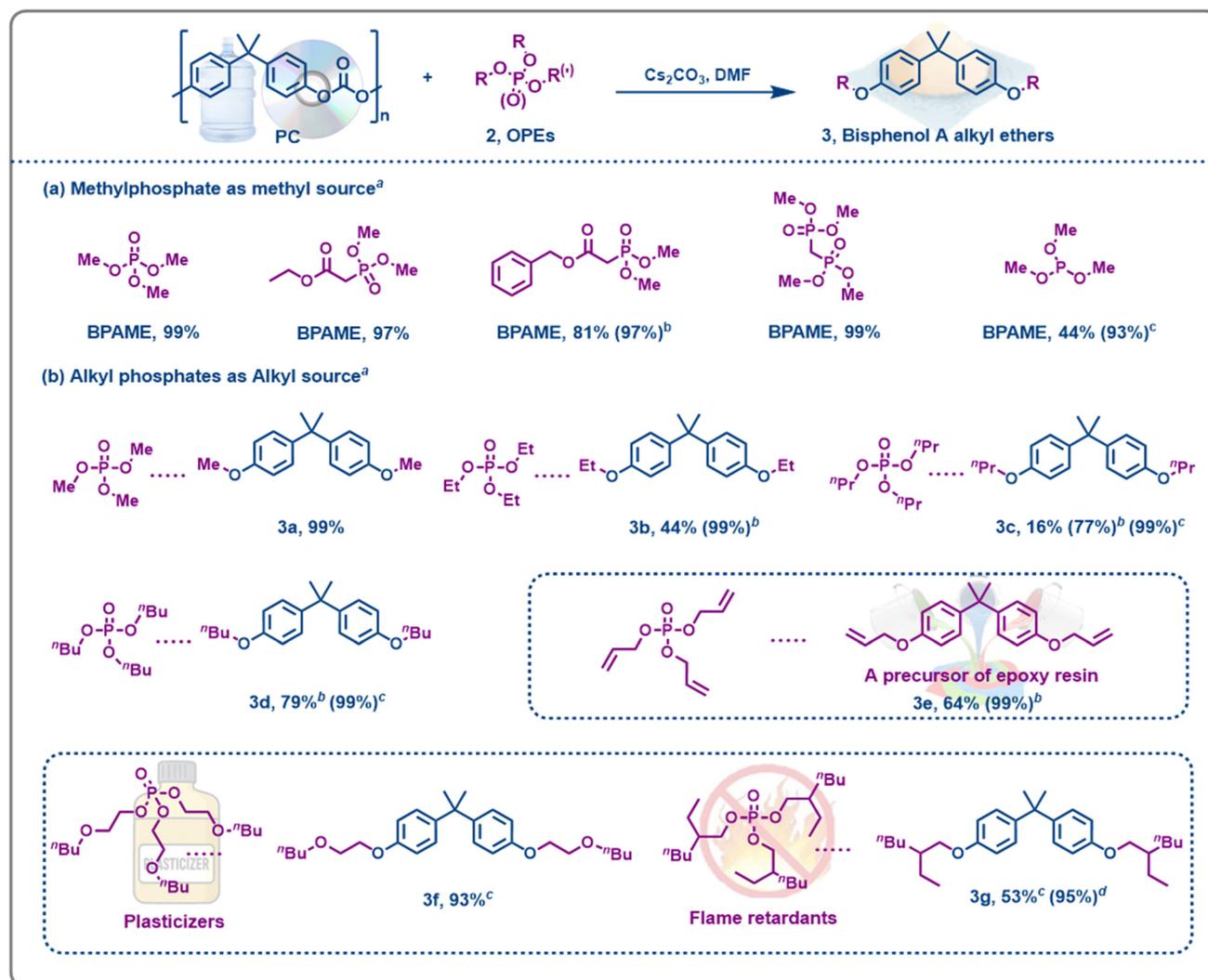
Fig. 2 Substrate scope of phosphate esters. (a) Methyl phosphate esters and (b) higher alkyl phosphate esters evaluated as alkylating agents. [a]Standard conditions: PC (1 mmol PC unit), Cs$_2$CO$_3$ (3 mmol), OPEs (3 mmol), DMF (2 mL), 100 °C, 30 min; [b]at 140 °C for 30 min; [c]at 140 °C for 5 h; and [d]at 160 °C for 7 h. The corresponding dealkylated phosphate ester products were detected with yields comparable with those of the BPA alkyl ethers and are therefore omitted for clarity.

cate polymer recycling and necessitate costly separation steps, can instead be directly converted *in situ* into value-added functional products. This dual valorization of both the polymer matrix and embedded additives enhances the practical applicability, process simplicity, and economic attractiveness of the co-upcycling strategy for an additive-rich plastic waste.

3.2 Real-world PC waste applicability

To validate the practical viability of this system, we applied both the PC-TMP (trimethyl phosphate) and PC-TAP (triallyl phosphate) systems to various discarded PC products representing the breadth of real-world waste streams. The adaptability of this approach was confirmed with a range of post-consumer PC waste feedstocks, including light tubes, transparent plates, blue buckets, flame-retardant shells, optical disks, and insulation sheets (Fig. 3a). For the PC-TMP system, these PC wastes, in the form of cropped pieces, were effectively co-processed with TMP and converted to BPAME with yields of 94%–98% under standard conditions (100 °C, 30 min). For the PC-TAP system, the corresponding BPAAE was obtained with yields of 92%–98% at 140 °C. This consistency across diverse waste sources, including those containing colorants, flame retardants, and plasticizers, demonstrates the robustness of the method toward compositional heterogeneity of post-consumer PC waste. Critically, this performance validation establishes that the system can accommodate the heterogeneity inherent in actual waste streams, a prerequisite for industrial implementation. By adjusting key parameters, such as catalyst composition, temperature, and reaction time, the process achieves wide substrate generality, enabling the valorization of diverse commercial PC wastes and OPE streams into valuable bisphenol A alkyl ethers.

Commercial PC materials often contain various additives, including stabilizers, plasticizers, pigments, and flame retardants, which could potentially influence the reaction system depending on their chemical properties. To evaluate their impact, we examined several representative additives commonly used in PC materials: a mold release agent (pentaerythrityl tetrastearate), a flame retardant (decabromodiphenyl ether), and a chain-terminating agent (*p-tert*-butylphenol). These additives had a negligible influence on the PC-TMP system, with the BPAME yield remaining at approximately 99% (Table S3). These observations indicate that the reaction system exhibits substantial tolerance toward typical additives present in commercial PC materials, likely arising from the chemical inertness of these additives under the reaction conditions, which precludes interference with depolymerization or alkyl transfer processes. This finding rationalizes the broad applicability observed above and confirms effective valorization of diverse commercial PC wastes.

Additionally, gram-scale experiments (10 g) were conducted using discarded optical disks to demonstrate preparative-scale feasibility (Fig. 3b). The solution turned brown during the reaction due to the dissolution of a dye coating present on the disk surface. After filtration, water and ethyl acetate were added, and BPAME was extracted into the organic phase. The

ethyl acetate solution containing BPAME was concentrated by rotary evaporation to afford crude BPAME, which was subsequently purified by recrystallization from methanol to yield 9.2 g of pure BPAME (91% isolated yield). ^{1}H NMR and ^{13}C NMR analyses (sections S6 and S7 in SI) confirmed complete methylation, with no detectable monomethylated intermediates, affording BPAME with a purity exceeding 99%. These results validate the quantitative conversion and highly selective double alkylation at the preparative scale. This gram-scale demonstration bridges the gap between laboratory proof-of-concept and the potential industrial application of the proposed co-upcycling strategy.

3.3 Practical implementation with realistic industrial waste streams

To assess the practical applicability of the proposed co-upcycling strategy, two representative industrial scenarios were investigated: (i) co-upcycling of waste PC with TOP-containing solvent waste generated from the anthraquinone process used for H_2O_2 production (Fig. 4a), and (ii) co-upcycling of waste PC with the TBP-based extraction waste from metallurgical operations (Fig. 4b). In the anthraquinone-based H_2O_2 production process, TOP is widely employed as a solvent owing to its high solubility for anthraquinone, favorable H_2O_2-solvent distribution coefficient, as well as high boiling and flash points.[43] During the solvent cycling process, waste liquids containing significant amounts of TOP are inevitably generated. These waste liquids primarily consist of TOP solvent, anthraquinone and its degradation products, and trace metal catalysts. Consequently, the co-upcycling of PC and TOP waste liquid from the anthraquinone process for H_2O_2 production is directly relevant to existing industrial processes. Using a mixture of waste PC and simulated TOP waste liquid, the co-upcycling reaction was performed, and the products were recovered through straightforward separation steps, including extraction, evaporation, and recrystallization. Bisphenol A dioctyl ether was obtained in 91% yield with high purity, demonstrating the technical feasibility of the approach. In the metallurgical industry, TBP is commonly used as an extractant for rare-earth elements, generating waste streams containing diluents, modifiers, and complexed metal ions.[44] We performed the co-processing of waste PC with simulated TBP-containing extraction liquid from metallurgical operations. Following simple processes, such as extraction, evaporation, and recrystallization, we obtained 87% yield of bisphenol A dibutyl ether. These results confirm that the proposed strategy is directly applicable to the co-upcycling of PC and high-concentration OPE waste streams encountered in metallurgical extraction processes.

3.4 Mechanistic origin of synergistic co-upcycling

Using the PC–TMP system as a model, we investigated the kinetic behavior and mechanistic basis of the synergistic co-upcycling process. Time-resolved analysis of the reaction (Fig. 5a) revealed the sequential formation of two intermediates, BPA and MMEP, with distinct temporal profiles. BPA con-
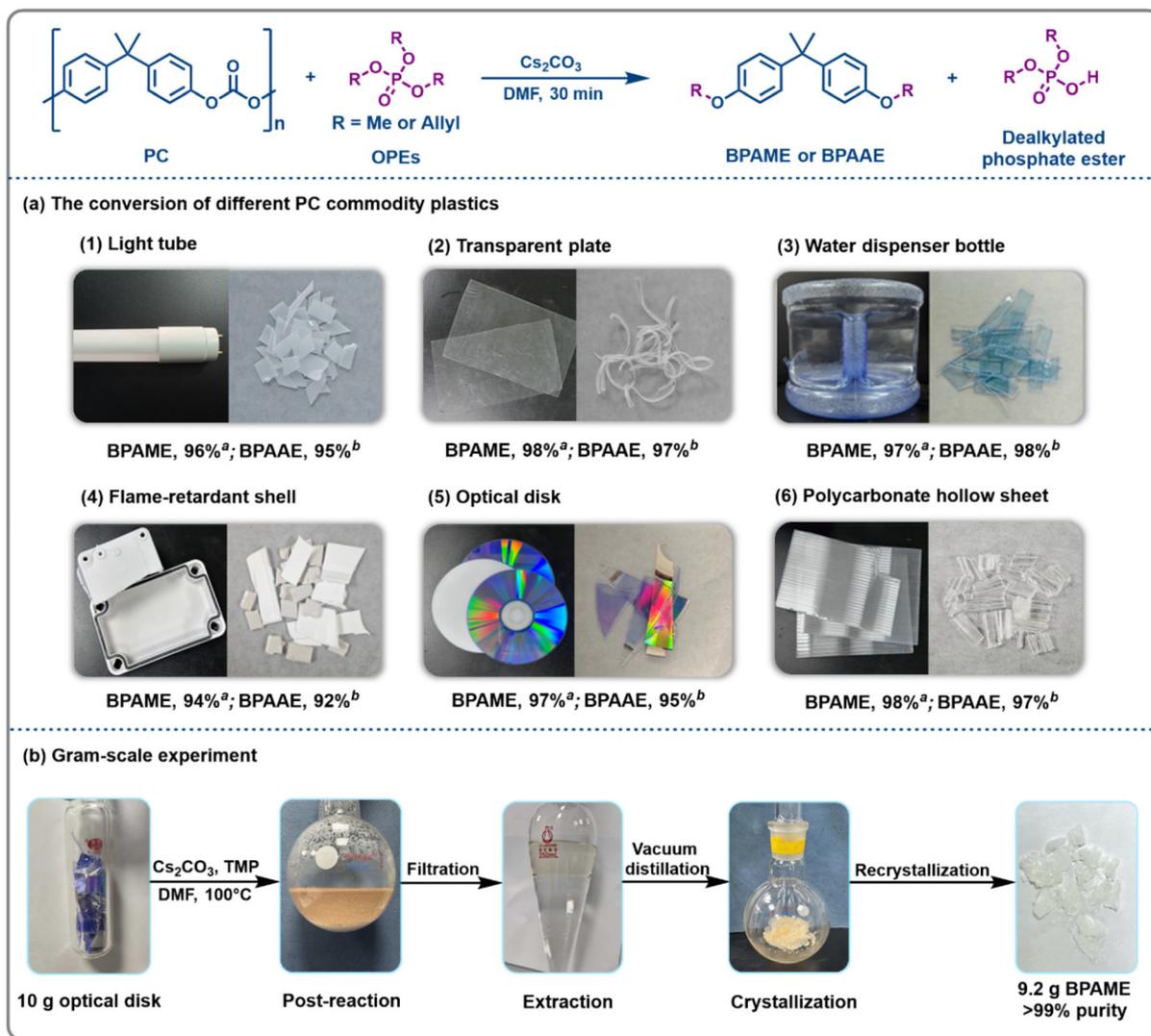
Fig. 3 Real-world PC waste applicability. (a) Conversion of various PC commodity plastics to BPAME *via* the PC–TMP system and BPAAE *via* the PC–TAP system. (b) Gram-scale experiment for the PC–TMP system. Reaction conditions: PC waste (1 mmol PC unit), Cs_2CO_3 (3 mmol), OPEs (3 mmol), DMF (2 mL), [a]100 °C for PC-TMP or [b]140 °C for PC-TAP, and 30 min.

centration reached a maximum at approximately 2.5 h, followed by the accumulation of MMEP at around 5 h, consistent with a stepwise transformation pathway: PC → BPA → MMEP → BPAME.

To quantify the origin of the observed synergy, the kinetics of three systems were compared: (i) PC depolymerization in the absence of TMP, (ii) direct methylation of BPA with TMP, and (iii) the combined PC–TMP system (Fig. 5b). BPA methylation was found to proceed substantially faster than PC depolymerization, indicating that PC depolymerization constitutes the rate-determining step. It was observed that PC depolymerization alone plateaued at a BPA yield of approximately 92%, reflecting an equilibrium limitation. In contrast, the introduction of TMP increased the overall BPAME yield to 99% by continuously consuming BPA as it formed, thereby driving the depolymerization equilibrium forward. This coupling effect

underpins the synergistic behavior: neither waste stream undergoes complete conversion independently, whereas their integration enables near-quantitative transformation.

Having established the kinetic basis for synergy, we next examined the catalytic role of carbonates in enabling this coupled transformation. Control experiments (Table S4) indicate that the carbonate plays a dual role in the reaction system. In the absence of Cs_2CO_3, no PC depolymerization occurred, confirming that carbonate is essential for initiating cleavage of the ester group. Furthermore, methylation of BPA with TMP did not proceed without Cs_2CO_3, whereas efficient alkyl transfer occurred in its presence. These results demonstrate that carbonate not only catalyzes PC depolymerization but also facilitates the formation of BPA-derived phenolate species, which serve as active nucleophiles in the subsequent alkyl transfer step. The role of carbonate activation in facilitating PC
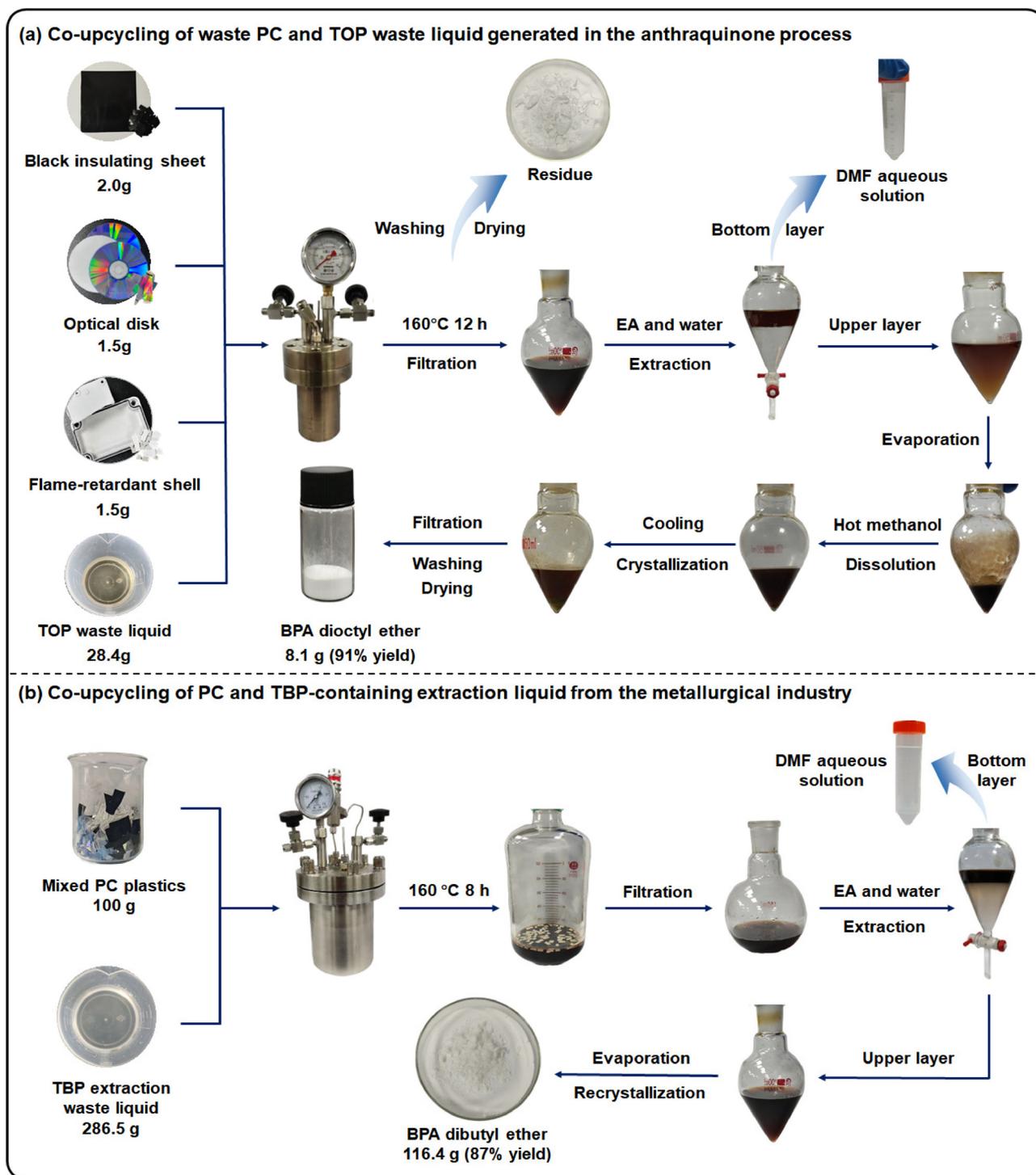
Fig. 4 Practical implementation with realistic industrial waste streams. Process flow diagram for the co-upcycling of PC with TOP-containing (a) and TBP-containing (b) industrial waste liquids. Reaction conditions: (a) PC waste (5 g, 19.7 mmol), Cs_2CO_3 (59.2 mmol), TOP-containing waste liquid (59.2 mmol), DMF (40 mL), 160 °C, and 12 h and (b) PC waste (100 g, 394 mmol), Cs_2CO_3 (787 mmol), TBP-containing waste liquid (905 mmol), DMF (800 mL), 160 °C, and 8 h.

depolymerization was further examined using crown ether additives (Fig. 5c). The addition of 15-crown-5 to Na_2CO_3 increased the BPAME yield from 5% to 70%, while 18-crown-6 enhanced the performance of K_2CO_3 from 73% to 99%. These results are consistent with the size-selective cation complexation,[45,46] which promotes carbonate ionization and enhances its nucleophilicity, thereby accelerating PC activation.
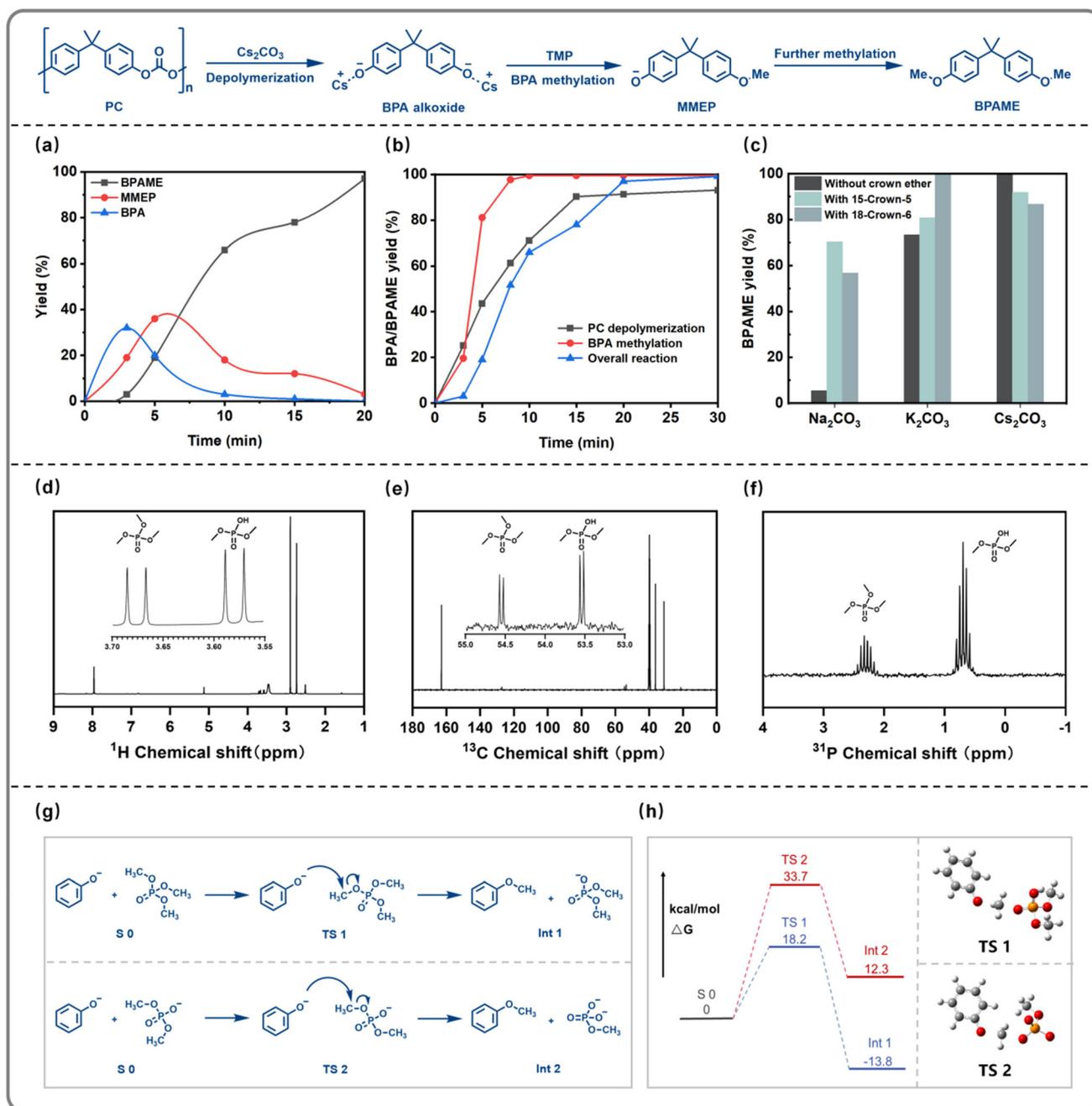
Fig. 5 Kinetics and mechanism. (a) Temporal evolution of the intermediates (BPA and MMEP) and product (BPAME) during the PC–TMP reaction. (b) Comparative kinetics of the individual reaction steps: PC depolymerization in the absence of TMP, BPA methylation in the absence of PC, and overall PC-to-BPAME conversion. (c) Effect of carbonate bases and crown ether additives on the BPAME yield. NMR characterization of the PC-TMP reaction products: (d) ^1H NMR, (e) ^{13}C NMR, and (f) ^{31}P NMR spectra. (g) Corresponding reaction schemes for phenoxide with TMP and DMP. (h) DFT-calculated activation barriers for the nucleophilic attack of phenoxide on TMP *vs.* DMP. Standard reaction conditions: PC (1 mmol PC unit), Cs$_2$CO$_3$ (3 mmol), TMP (3 mmol), DMF (2 mL), 100 °C, and 30 min.

Collectively, these findings support a two-stage reaction mechanism. In the first step, PC undergoes base-promoted depolymerization to generate BPA phenolate species. In the second step, these *in situ*-generated phenolates react with OPEs *via* nucleophilic substitution (S$_N$2) at the electrophilic alkyl groups bound to the phosphate center, proceeding through the P–O–C bond cleavage. This alkyl transfer produces BPA alkyl ethers while converting OPEs into partially dealkylated phosphate products. This sequential yet interconnected pathway integrates polymer depolymerization with *in situ* functionalization, establishing the mechanistic foundation for the waste-to-waste co-upcycling process.

A further distinguishing feature of the system is the controlled and selective mono-dealkylation of OPEs. When TMP is employed, it is selectively converted to dimethyl phosphate (DMP), a valuable industrial intermediate used in the synthesis of flame retardants, pharmaceuticals, agrochemicals, and ionic liquid precursors.[47,48] In contrast, in the PC–TMP co-upcycling system, TMP simultaneously functions as the alkylating agent for BPA and undergoes selective mono-demethylation to DMP. NMR spectroscopy confirmed DMP formation (Fig. 5d–f) with characteristic methyl proton signals at 3.57–3.59 ppm (^{1}H), methyl carbon signals at 53.51–53.56 ppm (^{13}C), and phosphorus signals at 0.59–0.80 ppm (^{31}P). Importantly, no signals corresponding to MMP or further dealkylated species were detected, indicating quantitative mono-dealkylation selectivity.

Density functional theory (DFT) calculations using phenoxide as a model nucleophile (Fig. 5g and h) provide a mechanistic rationale for the observed selectivity. Thermodynamically, the first demethylation step is favorable, with a negative Gibbs free energy change ($\Delta G < 0$), whereas the second demethylation step is associated with a positive Gibbs free energy change ($\Delta G > 0$) and is therefore thermodynamically disfavored. This intrinsic energetic asymmetry dictates that single demethylation is favored while suppressing further demethylation, accounting for the exclusive formation of the mono-demethylated product. From a kinetic perspective, the activation barrier for the first demethylation step (18.2 kcal mol^{-1}) is substantially lower than that for the second demethylation (33.7 kcal mol^{-1}), rendering further alkyl removal kinetically inaccessible under the reaction conditions. The combined thermodynamic and kinetic constraints thus enforce complete selectivity toward dimethyl phosphate (DMP), preventing over-demethylation. As a result, DMP is obtained with 100% selectivity, obviating the need for downstream purification and enabling the direct production of pure DMP alongside BPAME.

4. Conclusions

This work reports a synergistic co-upcycling strategy that chemically couples waste polycarbonate (PC) plastics with organophosphate esters (OPEs), two hazardous streams typically managed through separate and energy-intensive routes, in a single catalytic process. Using mild carbonate catalysts, PC can be completely depolymerized while the released bisphenol A (BPA) is selectively alkylated, with OPEs serving as *in situ* alkylating agents. The one-pot system shows broad generality across diverse commercial PC wastes and OPEs, affording bisphenol A alkyl ethers in consistently high yields (92%–99%). Importantly, the strategy remains effective in chemically complex, high-concentration matrices representative of industrial solvent wastes, including the TOP-based solvent waste from anthraquinone H_2O_2 production and TBP-based extraction waste from metallurgical operations, underscoring its practical relevance for solvent-rich residues. A distinguishing feature is the controlled mono-dealkylation of OPEs, exemplified by the quantitative conversion of trimethyl phosphate to dimethyl phosphate without over-dealkylation, enabling concurrent recovery of an industrially valuable phosphate intermediate. Overall, this study demonstrates a waste-to-waste co-upcycling approach that leverages chemical complementarity to reduce environmental burdens while recovering chemical value.

Author contributions

Yunkai Yu: experiment conduction, formal analysis, and writing – original draft. Zexiang Wu: formal analysis and writing – review and editing. Minghao Zhang: formal analysis and writing – review and editing. Siyu Zhang: formal analysis. Yanwen Wang: DFT calculations. Jing Li: formal analysis. Weixiang Wu: formal analysis. Qingqing Mei: conceptualization, formal analysis, funding acquisition, resources, supervision, and writing – review and editing.

Conflicts of interest

The authors declare no competing interests.

Data availability

The data supporting this article have been included as part of the supplementary information (SI). Supplementary information is available. See DOI: https://doi.org/10.1039/d6gc01199c.

Acknowledgements

References

1 P. Stegmann, V. Daioglou, M. Londo, D. P. Van Vuuren and M. Junginger, *Nature*, 2022, **612**, 272–276.
2 X. Gao, Z. Wang, M. Zhang, Y. Yu, S. Zhang and Q. Mei, *Angew. Chem., Int. Ed.*, 2025, **64**, e202513723.
3 J. Wang, J. Jiang, X. Dong, Y. Zhang, X. Yuan, X. Meng, G. Zhan, L. Wang, Y. Wang and A. J. Ragauskas, *Green Chem.*, 2022, **24**, 8562–8571.
4 X. Yuan, N. M. Kumar, B. Brigljević, S. Li, S. Deng, M. Byun, B. Lee, C. S. K. Lin, D. C. W. Tsang, K. B. Lee, S. S. Chopra, H. Lim and Y. S. Ok, *Green Chem.*, 2022, **24**, 1494–1504.

5 Z.-N. Wang, X.-X. Xiao, Y. Gong, T.-Y. Bai, J.-H. Bai, H.-B. Zhao, L. Chen, B.-W. Liu and Y.-Z. Wang, *Chem. Eng. J.*, 2025, **515**, 163503.

6 C. Shi, W. T. Diment and E. Y.-X. Chen, *Angew. Chem.*, 2024, **136**, e202405083.

7 C. Symeonides, K. Vacy, S. Thomson, S. Tanner, H. K. Chua, S. Dixit, T. Mansell, M. O'Hely, B. Novakovic, J. B. Herbstman, S. Wang, J. Guo, J. Chia, N. T. Tran, S. E. Hwang, K. Britt, F. Chen, T. H. Kim, C. A. Reid, A. El-Bitar, G. B. Bernasochi, L. M. D. Delbridge, V. R. Harley, Y. W. Yap, D. Dewey, C. J. Love, D. Burgner, M. L. K. Tang, P. D. Sly, R. Saffery, J. F. Mueller, N. Rinehart, B. Tonge, P. Vuillermin, the BIS Investigator Group, F. Collier, A.-L. Ponsonby, L. C. Harrison, S. Ranganathan, L. Gray, A.-L. Ponsonby and W. C. Boon, *Nat. Commun.*, 2024, **15**, 6367.

8 C. Jehanno, J. W. Alty, M. Roosen, S. De Meester, A. P. Dove, E. Y.-X. Chen, F. A. Leibfarth and H. Sardon, *Nature*, 2022, **603**, 803–814.

9 S. Zhang, Q. Hu, Y.-X. Zhang, H. Guo, Y. Wu, M. Sun, X. Zhu, J. Zhang, S. Gong, P. Liu and Z. Niu, *Nat. Sustain.*, 2023, **6**, 965–973.

10 Q. Zhang, N. Wang, C. Hu, P.-Y. Li, F.-Q. Bai, X. Pang, X. Chen and X. Wang, *Green Chem.*, 2024, **26**, 11976–11983.

11 M.-J. Zhou, Y. Gu, Y. Chen, W. Bian, Y. Hu, Y. Yu and Y. Xie, *J. Am. Chem. Soc.*, 2026, **148**, 7482–7494.

12 N. Hu, L. Su, H. Li, N. Zhang, Y. Qi, H. Wang, X. Cui, X. Hou and T. Deng, *Green Chem.*, 2024, **26**, 9378–9387.

13 L. Trullemans, S.-F. Koelewijn, I. Boonen, E. Cooreman, T. Hendrickx, G. Preegel, J. Van Aelst, H. Witters, M. Elskens, P. Van Puyvelde, M. Dusselier and B. F. Sels, *Nat. Sustain.*, 2023, **6**, 1693–1704.

14 S. T. Nguyen, E. A. McLoughlin, J. H. Cox, B. P. Fors and R. R. Knowles, *J. Am. Chem. Soc.*, 2021, **143**, 12268–12277.

15 N. Moyilla, G. Padhi, D. Kalsi and N. Barsu, *ACS Sustainable Chem. Eng.*, 2024, **12**, 18362–18372.

16 Y. Huang, J. Xie, Y. Zhou, Q. Song, Y. Lei, C. Zhou, C. Wang, K. Ma, L. Song, H. Yue and J.-J. Zou, *Green Chem.*, 2026, **28**, 415–423.

17 J. Wang, D. Li, Z. Zhang, Z. Zhuang, J. Yang, S. Wang, T. Gan, D. Wang and J. Jiang, *Angew. Chem., Int. Ed.*, 2026, e24681.

18 M. Zhang, Y. Bai, Z. Wang, X. Gao, W. Zhang, J. Li, W. Wu, H. Zhou and Q. Mei, *Chem. Eng. J.*, 2024, **500**, 156914.

19 J. I. Van Der Vlugt, M. M. P. Grutters, A. M. Mills, H. Kooijman, A. L. Spek and D. Vogt, *Eur. J. Inorg. Chem.*, 2003, **2003**, 4361–4369.

20 H. Chen, Y. Yin, G. Wang, X. Xiao, X. Jiang and M. Feng, *Angew. Chem., Int. Ed.*, 2025, **64**, e20251261.

21 Y. Sun, X. Han, W. Liu, Z. Shi, Y. Zhang, C. Chen, Q. Chen, T. Jia, T. Mao and F. Yin, *Chem. Eng. J.*, 2025, **505**, 159187.

22 Z. Xie, P. Wang, X. Wang, J. Castro-Jiménez, R. Kallenborn, C. Liao, W. Mi, R. Lohmann, M. Vila-Costa and J. Dachs, *Nat. Rev. Earth Environ.*, 2022, **3**, 309–322.

23 M. Han, K. Yu, R. Zhang, B. Chen, M. Xiong, Y. Kang, X. Yu, Z. Qin and X. Xu, *Environ. Sci. Technol.*, 2025, **59**, 24538–24552.

24 K. D. Demadis, S. K. Adla, J. Timonen and P. A. Turhanen, *Green Chem.*, 2025, **27**, 863–914.

25 J. Zhang, S. Wang, X. Chen, W. Zhao and L. Su, *Chem. Eng. J.*, 2026, **527**, 171764.

26 S. Wang, J. Qian, B. Zhang, L. Chen, S. Wei and B. Pan, *Environ. Sci. Technol.*, 2023, **57**, 1907–1918.

27 T. Liu, Y. Zhang, Z. Shan, M. Wu, B. Li, H. Sun, G. Su, R. Wang and G. Zhang, *Nat. Water*, 2023, **1**, 1059–1067.

28 Y. Xiang, Y. Liu, B. Cong, Z. Cai, N. Wang, H. Zhang, C. He and B. Lai, *Water Res.*, 2024, **267**, 122494.

29 M. Fan, P. Zhang, C. Wang, J. Tang and H. Sun, *J. Hazard. Mater.*, 2022, **428**, 128254.

30 M. J. Frisch, G. W. Trucks, H. B. Schlegel, G. E. Scuseria, M. A. Robb, J. R. Cheeseman, G. Scalmani, V. Barone, G. A. Petersson, H. Nakatsuji, X. Li, M. Caricato, A. V. Marenich, J. Bloino, B. G. Janesko, R. Gomperts, B. Mennucci, H. P. Hratchian, J. V. Ortiz, A. F. Izmaylov, J. L. Sonnenberg, D. Williams-Young, F. Ding, F. Lipparini, F. Egidi, J. Goings, B. Peng, A. Petrone, T. Henderson, D. Ranasinghe, V. G. Zakrzewski, J. Gao, N. Rega, G. Zheng, W. Liang, M. Hada, M. Ehara, K. Toyota, R. Fukuda, J. Hasegawa, M. Ishida, T. Nakajima, Y. Honda, O. Kitao, H. Nakai, T. Vreven, K. Throssell, J. A. Montgomery Jr, J. E. Peralta, F. Ogliaro, M. J. Bearpark, J. J. Heyd, E. N. Brothers, K. N. Kudin, V. N. Staroverov, T. A. Keith, R. Kobayashi, J. Normand, K. Raghavachari, A. P. Rendell, J. C. Burant, S. S. Iyengar, J. Tomasi, M. Cossi, J. M. Millam, M. Klene, C. Adamo, R. Cammi, J. W. Ochterski, R. L. Martin, K. Morokuma, O. Farkas, J. B. Foresman and D. J. Fox, *Gaussian 16, Revision C.01*, Gaussian, Inc., Wallingford CT, 2016.

31 R. Krishnan, J. S. Binkley, R. Seeger and J. A. Pople, *J. Chem. Phys.*, 1980, **72**, 650–654.

32 A. D. McLean and G. S. Chandler, *J. Chem. Phys.*, 1980, **72**, 5639–5648.

33 T. Clark, J. Chandrasekhar, G. W. Spitznagel and P. V. R. Schleyer, *J. Comput. Chem.*, 1983, **4**, 294–301.

34 M. J. Frisch, J. A. Pople and J. S. Binkley, *J. Chem. Phys.*, 1984, **80**, 3265–3269.

35 L. E. Roy, P. J. Hay and R. L. Martin, *J. Chem. Theory Comput.*, 2008, **4**, 1029–1031.

36 Y. Chen, P. Qiu, H. Sun, L. Sun and Z. Liu, *Appl. Organomet. Chem.*, 2022, **36**, e6860.

37 K. Fukui, *Acc. Chem. Res.*, 1981, **14**, 363–368.

38 S. Hu and A. T. Radosevich, *Angew. Chem., Int. Ed.*, 2024, **63**, e202409854.

39 A. S. Trita, L. C. Over, J. Pollini, S. Baader, S. Riegsinger, M. A. R. Meier and L. J. Gooßen, *Green Chem.*, 2017, **19**, 3051–3060.

40 T. Rukkijakan, S. Akkarasamiyo, S. Sawadjoon and J. S. M. Samec, *J. Org. Chem.*, 2018, **83**, 4099–4104.

41 A. Qadeer, M. Anis, G. R. Warner, C. Potts, G. Giovanoulis, S. Nasr, D. Archundia, Q. Zhang, Z. Ajmal, A. C. Tweedale, W. Kun, P. Wang, R. Haoyu, X. Jiang and W. Shuhang, *Green Chem.*, 2024, **26**, 5635–5683.

42 S. Khodavandegar and P. Fatehi, *Green Chem.*, 2024, **26**, 10070–10086.

43 S.-A. Theofanidis, A. G. Georgiadis, C. J. W. Hop, X. Yu, V.-L. Yfanti, G. Fayet, C. Villemur, H. Vleeming, E. Delikonstantis and R. H. Heyn, *ACS Omega*, 2025, **10**, 61076–61095.

44 L. Cui, L. Wang, M. Feng, L. Fang, Y. Guo and F. Cheng, *Green Energy Environ.*, 2021, **6**, 607–616.

45 J. Mai, J. Maurer, J. Langer and S. Harder, *Nat. Synth.*, 2023, **3**, 368–377.

46 T. N. Poe, H. Ramanantoanina, J. M. Sperling, H. B. Wineinger, B. M. Rotermund, J. Brannon, Z. Bai, B. Scheibe, N. Beck, B. N. Long, S. Justiniano, T. E. Albrecht-Schönzart and C. Celis-Barros, *Nat. Chem.*, 2023, **15**, 722–728.

47 V. Amani and M. Rafizadeh, *J. Mol. Struct.*, 2021, **1229**, 129834.

48 Z. Wang, Z. Su, Y. Xu, J. Qi, B. Qi, X. Wei, X. Chen, Y. Hu, Z. Liu and X. Guo, *ACS Sustainable Chem. Eng.*, 2024, **12**, 14087–14098.